Investigation of Temperature-Dependent Photoluminescence Mechanisms in Porous Silicon Layer for Optoelectronic Devices

I. Tifouti[a,*], B. Meriane[a], S. Rahmouni[a], N. Boukhanoufa[b] and H. Bendjeffal[a]

[a] *Laboratory of Physical Chemistry and Biology of Materials, Higher Normal School of Technological Education ENSET, Bousta St., 21000, Skikda, Algeria*
[b] *Electronic Department, University of Batna, Fesdis St., 05000, Batna, Algeria*

Received: 12.02.2025 & Accepted: 23.04.2025

Doi: 10.12693/APhysPolA.147.449 *e-mail: issam86@yahoo.fr

This study examines how the variation of temperature affects the photoluminescence properties of porous silicon, offering insights into surface, defects, and carrier dynamics interactions. Porous layers are obtained using an electrochemical method, revealing two notable photoluminescence emission peaks. The study suggests two different non-radiative recombination processes based on intensity changes with temperature. Surface conditions contribute to the thermal quenching of the photoluminescence at low temperatures (10–60 K), while non-radiative recombination is linked to the thermal escape of excitons at higher temperatures (60–300 K). A comprehensive understanding of these processes is essential for effective integration of optoelectronic devices.

topics: porous silicon (PSi), photoluminescence (PL), optoelectronic, low temperature

1. Introduction

The production of porous silicon (PSi) layers via electrochemical etching facilitates scalable manufacturing techniques, making it a cost-effective and widely applicable solution. Owing to its unique properties, PSi is extensively used in diverse fields, including biological membranes [1], 3D photonic crystals [2], gas sensors [3–5], biosensors, micromachining [6], biomedical applications [7], photoluminescence, and solar cells [8–11], as well as in photovoltaics and optoelectronic devices [8, 9, 12–14]. Efforts to enhance PSi properties through various modifications remain an active area of research [15, 16].

Numerous studies have investigated PSi, including Canham's seminal work on photoluminescence (PL) phenomena [17], which introduced theories explaining the mechanisms behind PL formation. Quantum confinement effects in PSi [10] allow tuning of electrical and optical properties by controlling the size of silicon nanostructures, making the material invaluable for a wide range of electronic and optoelectronic applications [18]. The quantum confinement model attributes light emission to smaller PSi crystallites, while the high surface-to-volume ratio of PSi increases its susceptibility to chemical degradation, fragility, and oxidation [19]. These characteristics are used in photodetectors and high-efficiency light-emitting diodes (LEDs).

This study aims to investigate the influence of temperature on the photoluminescence properties of PSi layers fabricated from N-type silicon substrates. The study explores recombination processes and emission peak origins by analyzing PL data. Observations of PL behavior at varying temperatures reveal critical insights into the optical and electronic properties of PSi.

Porous silicon, with its distinctive optical and electrical attributes, holds promise for applications in sensors, optoelectronics, and photovoltaics [20, 21]. Understanding its temperature-dependent PL characteristics provides a deeper understanding of the material's behavior, enabling further optimization for advanced technological applications.

2. Experimental details

2.1. Materials and chemicals

The wafers used in the experiment are type N(100) with a resistivity of 3–5 Ω cm. They have a thickness of 625 ± 75 μm. The wafers were cleaned with ethanol, followed by cleaning before each experiment and then drying with nitrogen.

2.2. Porous silicon preparation and photoluminescence (PL) measurements

In this study, electrochemical etching was used to generate samples of porous silicon. The Si samples were subjected to a special cleaning technique before being placed in a Teflon electrochemical cell. The cell was filled with 100 mL of electrolyte solution prepared by mixing C_2H_5OH (98%) and HF solution (40%) in a 1:1 volume ratio. The samples were illuminated during preparation [10]. An ethanol solution was used to create uniform porous silicon layers and to minimize the visibility of H_2 bubbles on the surface. This ensured that the PSi layers were uniform. After 30 min of etching, a rounded surface was successfully formed within an anodized porous silicon shell. The area of this circular surface was 0.64 cm^2. Figure 1 shows the schematic details of the electrochemical cell used, including the anodized shell. As mentioned above, the cell was connected to a reliable power source to ensure a constant and uninterrupted power supply. The Si samples have a metal electrode on their back, which is isolated from the HF/ethanol electrolyte by an inactive HF O-ring. Therefore, only the outer surface is exposed to the corrosive effects of the electrolyte. The size of the O-ring directly determines the diameter of the resulting PSi surface. This relationship is important when marginal effects are not taken into account. In order to obtain a uniform structure and to control the thickness and porosity of the films, the dissolution process was carried out by maintaining a constant electric current between the electrodes used [10, 21].

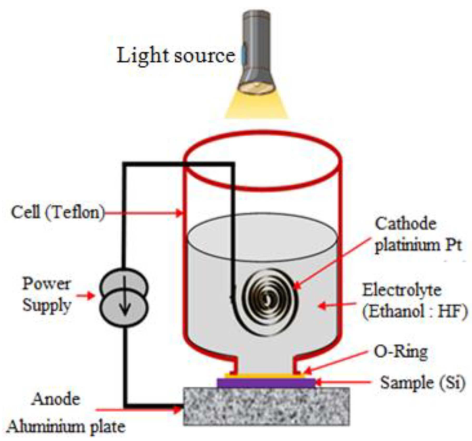

Fig. 1. Diagram of the electrochemical cell for producing porous silicon (PSi) films.

The temperature-dependent photoluminescence spectra were obtained using a solid-state laser with an excitation wavelength of 447 nm. The obtained data were recorded using an HR monochromator (Jobin Yvon) with a GaAs photomultiplier coupled to a conventional lock detector. The sample surface was exposed to a 7.66 mW laser.

3. Results and discussion

3.1. Photoluminescence study

As a function of temperature, the photoluminescence characteristics of N-doped porous silicon may exhibit intriguing behaviors. Porous silicon is a silicon variant characterized by an exceptionally porous structure; its optical characteristics are highly susceptible to variations in surface conditions, impurity content, and the structure of the material. The investigation of low-temperature photoluminescence is a prevalent methodology employed within the domains of condensed matter physics and materials science [22]. This technique quantifies the light emitted by a substance when exposed to photons at low temperatures [23, 24]. Our study aims to investigate the temperature-dependent variations in the PL band to understand the mechanisms of radiative recombination and gain insights into the characteristics of energy levels associated with PL. The study's main objective was to examine the build-up of intensity and variations in intensity in response to temperature in the range from 10 to 300 K. The silicon sample that was examined is classified as type N(100) and was exposed to the subsequent conditions: $t = 3$ min, [HF]-20%, and a current density of 25 mA/cm^2. The shift in the peak wavelength of the photoluminescence spectrum is directly influenced by temperature variations. The observed shift can be caused by the change in the band gap values of the porous silicon's energy due to material's thermal expansion, interactions between carriers and phonons, and quantum confinement effects.

Temperature can affect the band gap of porous N-type silicon. The temperature variations can lead to a change in the highest wavelength of the spectrum of photoluminescence. When the temperature rises, thermal energy impacts the band gap, which could change the photoluminescence spectra. It is possible to attribute the observed shift to many processes, such as the material's thermal expansion, the ways the carriers and phonons interact, and alterations in the energy band gap of porous silicon (PSi) caused by quantum-limited effects.

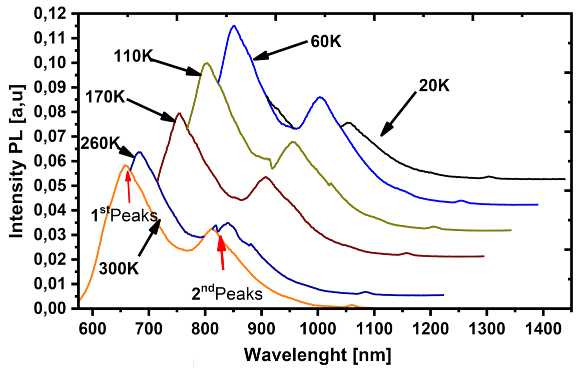

Fig. 2. Photoluminescence spectra of N(100) type porous silicon samples analyzed between 10 and 300 K.

However, non-radiative methods can reduce the intensity of photoluminescence, for example carriers at elevated temperatures or thermal excitation of surface states. At the same time, the photoluminescence spectrum of PSi at a temperature of 60 K frequently exhibits well-defined and more distinct emission peaks. The reason for this is the decreased thermal widening of energy levels, which enables a more accurate measurement of the energies of emission related to confinement effects inside the porous structure and other quantum electronic transitions. The photoluminescence spectra may produce peaks attributed to contaminants or defects in the porous silicon substance. Temperature may affect the emission resulting from this flaw. The temperature-dependent photoluminescence characteristics of PSi are influenced by the choice of excitation wavelength [25]. By varying the wavelengths used for excitation, different and distinct states within the PSi structure can be excited, resulting in changes in the observed photoluminescence spectra at various temperatures. In porous silicon layers, nanoscale structures frequently exhibit impacts of quantum confinement. At low temperatures, quantum confinement can result in distinct energy levels that impact the PL features [22, 26]. The dependence of photoluminescence on temperature can supply valuable insights into the quantum confinement behavior exhibited by optoelectronic devices [27]. Porous silicon's photoluminescence spectrum offers significant insights into the electronic structure and energy levels of the material [28]. The spectrum shown in Fig. 2 reveals an intense peak at 660 nm, primarily attributed to the absorbance of porous silicon, while the peak at 810 nm corresponds to the characteristics of the dopant. When certain impurities are added to the N-type substrate by doping the PL emission, the presence of dopant-related energy states can influence the spectrum. Dopant-related energy transitions within porous silicon structure can lead to the emergence of additional peaks in the PL spectrum. The existence of these states is a sign of the degree of doping and the particular dopants used. The study of PL emission provides significant insight into the electrical and optical properties of the material, making it an effective method for evaluating porous silicon structures at a temperature of 60 K. The photoluminescence spectra of porous silicon often show clear emission peaks and improved resolution. The reason for this phenomenon can be explained by the reduction in the energy level dispersion caused by thermal effects. This allows for a more precise measurement of the emission energies related to different electronic shifts in the porous material and the effects of quantum confinement [29]. The exact behavior may vary depending on the pore size and additional structural parameters, surface chemistry, and fabrication method. The luminescence capabilities at this low temperature can be significantly influenced by the functionality of the porous structure and the surface conditions.

3.2. Photoluminescence intensity evolution as a function of temperature

Temperature variations can affect the level of photoluminescence. Generally, an increase in temperature can cause a decrease in photoluminescence intensity. Higher temperatures often inhibit the radiative recombination process, which is mostly responsible for photoluminescence due to the increased prevalence of non-radiative recombination activities. In the same context, we wanted to study the different levels of intensity associated with different temperatures. It was found that there is a correlation between changes in intensity and temperature, which can be attributed to temperature-dependent generation and recombination rates of the carriers in the porous structure of the silicon material, as well as another unidentified reason [30]. The dominance of radiative recombination processes could lead to an increase in PL intensity at lower temperatures. On the other hand, at elevated temperatures, non-radiative mechanisms, such as thermal stimulation of surface charge states or carriers, can reduce the intensity level of photoluminescence [31].

The decrease in PL intensity (I_{PL}) with increasing temperature, especially below 50 K ($T < 50$ K), can be attributed to the process of exciton shift to a lower energy level by activation of non-radiative processes. An increased photoluminescence can be observed in the emission of the PSi layer. Within the temperature range of 50–60 K, decreasing temperatures lead to a decrease in non-radiative recombination processes, which in turn increases the carrier lifetime and promotes a higher number of instances of radiative recombination [32]. The assumption is that excitons trapped in the lowest localization states undergo thermal activation to move to higher states. This in turn leads to their radiative recombination. This mechanism ultimately leads to an increase in the intensity of the interband photoluminescence [33]. At a temperature of 60 K, the level of photoluminescence in PSi generally shows an enhancement compared to the standard room temperature of 300 K. This enhancement is due to the decrease in temperature, which reduces non-radiative recombination processes, resulting in longer carrier lifetimes and increasing the impact of radiative recombination. As a result, PL emission is stronger and spectral peaks can be more pronounced and well-defined. It is important to note that the properties of PSi at a temperature of 60 K can vary depending on the fabrication method, pore size, surface chemistry, and any relevant structural factors. At elevated temperatures (i.e., 60 K), the heat activation effect is enhanced, leading to the transformation of localized excitons into a free state and their dispersion throughout the structure without generating radiation. As a result, this event causes a decrease in the brightness of the photoluminescence [33]. At normal temperatures, PL intensity may be reduced due to increased thermal carrier excitation, potentially leading to more pronounced non-radiative recombination. At higher temperatures, the photoluminescence peaks may become broader and the emission intensity may decrease, in contrast to decreasing temperatures. Figure 3 shows a noticeable increase in PL intensity at a specific temperature known as TM-60 K.

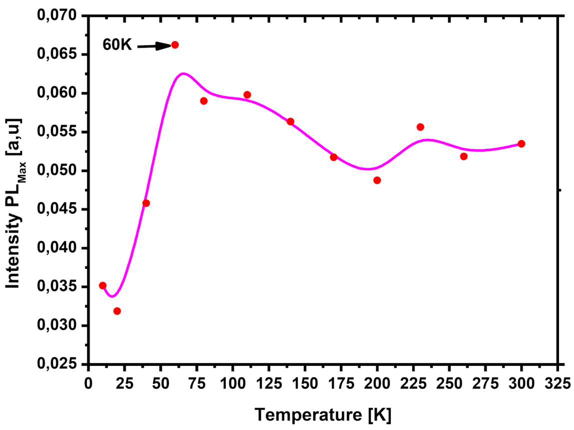

Fig. 3. Photoluminescence intensities evolution in a PSi film formed on N(100) substrate as a function of temperature.

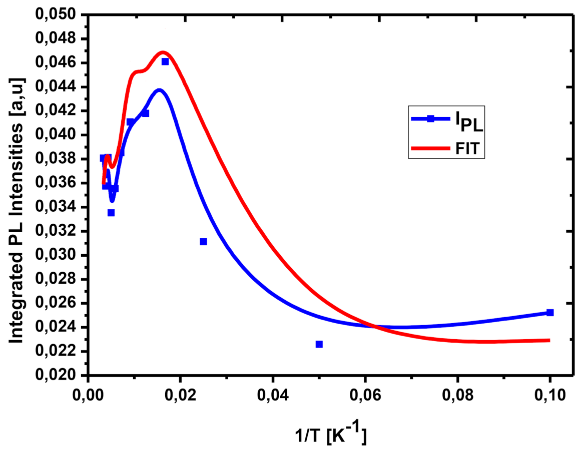

Fig. 4. Integrated photoluminescence intensity variation as a reciprocal temperature function.

3.3. Photoluminescence intensity versus reciprocal temperature

Quantum confinement phenomena can modify the energy difference between the valence and conduction bands in porous silicon structures. The band gap energy of silicon nanocrystals in the porous structure directly correlates to their size. As the nanocrystals decrease in size, the band gap energy increases. In addition, the band gap energy can also be affected by variations in the reciprocal temperature, thereby influencing photoluminescence emission characteristics. Based on studies by G.E. Weng et al. [34] and D. Zhao et al. [35], two different types of transfer processes have been discovered:

(i) The initial process is equivalent to a tunnel transfer [35, 36].

(ii) At lower temperatures, the second mechanism, referred to as dissociation by heat transfer [23], is not essential.

Nevertheless, it has been demonstrated that the variation of PL intensity with temperature is the reason why these two exciton injection techniques exist.

The experimental study by Ten et al. [37] showed that changing the temperature can accelerate the tunneling. In contrast, Jin Hua et al. [38] confirmed that the thermal dissociation of excitons is directly related to the increase in temperature. This phenomenon allows excitons to move more quickly from quantum dots (QDs) to quantum wells (QWs), which have lower energy levels [39, 40]. Figure 4 shows the relationship between the integrated photoluminescence intensity and the reciprocal temperature. Based on the transfer processes mentioned above, we used the two-energy model to fit the observed curve exactly. The two-energy model can be represented by

$$I_{\mathrm{PL}}(T) = I_{\mathrm{PL}}(0)\,\frac{1}{\left(1 + a_1 \exp\left(-\frac{e_1}{k_{\mathrm{B}}T}\right)\right)^2} \times \left[1 + A\frac{a_2 \exp\left(-\frac{e_2}{k_{\mathrm{B}}T}\right)}{1 + a_2 \exp\left(-\frac{e_2}{k_{\mathrm{B}}T}\right)}\right]. \quad (1)$$

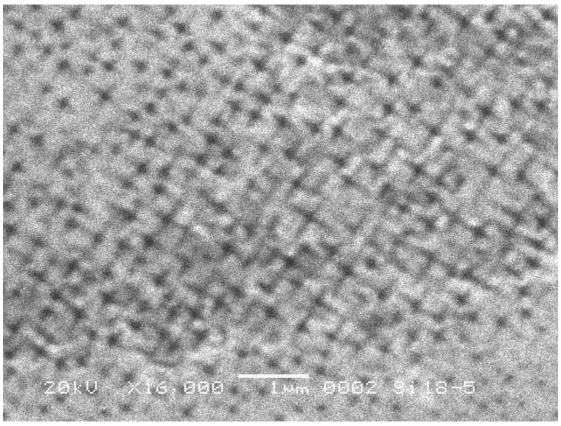

Fig. 5. SEM image of porous silicon surface grown from a type N(100) substrate.

TABLE I

Values obtained for parameters presented in (1).

Parameter	Value
I_{PL}	2.32×10^{-1}
e_1	$8.33 \times 10^{-5} \times 36.6 = 3.05$ meV
a_1	4.04×10^{-1}
A	1.72
e_2	$8.33 \times 10^{-5} \times 1205.84 = 100.44$ meV
a_2	11.54×10^{14}

The activation energy was determined by analyzing the spectrum using Origin Pro8. The variable e_1 represents the initial thermal activation energy, while e_2 indicates the subsequent thermal activation energy. The fixation parameters are denoted as A, a_1, and a_2. Table I and Fig. 4 show the relationship between the PL intensity values and the reciprocal temperature ($1/T$).

The inverse temperature relationship is due to the thermal activation of carriers. The thermal energy of carriers increases with temperature, which helps them overcome obstacles and participate in non-radiative recombination processes. An increase in temperature can lead to decreased PL intensity. For PL analysis as a function of temperature, this is the activation energy of charge carriers (electrons) from one energy level to other energy levels. The low-value energy e_2 is attributed to the energies of phonons in the material (related to thermal agitation). The energy e_1 may be related to the activation of carriers from one level to another. The obtained results suggest that the thermal activation energy for one energy level differs from that for an additional level. The observed behavior can be explained by the enhancement of the tunneling mechanism with increasing temperature [36]. The thermal activation energy of phonons in porous silicon has been previously documented. QDs have an impressive influence on the high-energy spectrum. The energy levels have distinct thermal activation energies. The presence of quantum confinement effects is a direct consequence of the nanoscale structure of porous silicon. The energy levels of the carriers are quantized due to the variations in the dimensions of the silicon nanocrystals within the porous structure. Temperature variations can alter the effects of quantum confinement and the quality of photoluminescence emission. The experimental research includes studying the correlation between the integrated PL intensity and the reciprocal temperature. The data patterns provide insight into the interaction of factors affecting the photoluminescence release in porous silicon.

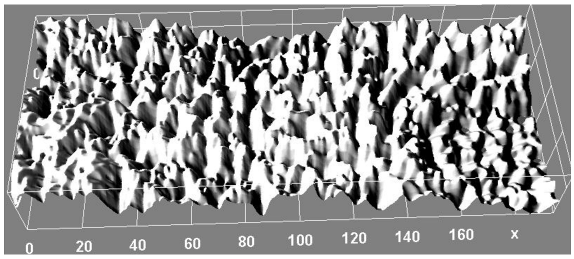

Fig. 6. Distribution of pores on porous silicon SEM images analyzed using ImageJ software.

3.4. Morphological studies

An in-depth analysis of the arrangement of porous silicon films on N(100) Si substrates provides a profound understanding of the material's physical properties. Using advanced techniques such as scanning electron microscopy (SEM), we could effectively view the porous structure at different depths, assess the range of pore diameters, and analyze the surface topography. An analysis of the relationship between the etching parameters provides valuable information on the influence of the manufacturing conditions. These results improve the understanding of the material's structure and provide a basis for raising the standard of manufacturing processes and exploring its applications.

SEM images show a uniform distribution of pores and homogeneous structure throughout the film. Nanoporous silicon films offer a unique feature. The pores are aligned parallel to the prescribed crystallographic orientation of the substrate (100) [41]. The alterations affect the width of the Si doping concentration depletion zone, which can influence the morphological variations. The number of pores created in the silicon type and the doping concentration (resistivity) determine the silicon surface as p-type or n-type. Figure 5 shows the surfaces, and Fig. 6 depicts clearly defined and uniform nanopores. The diameter of the sides is in the nanometre range. The presence of various

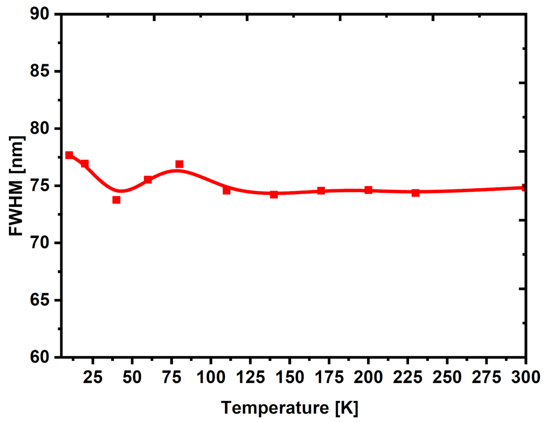

Fig. 7. FWHM as a function of temperature.

morphologies in other instances of porous silicon layers can be attributed to the silicon/electrolyte interface, which gives rise to a depletion zone resembling p–n junctions. In our specific scenario, the use of light on the nanoporous N-type silicon allows the control of pore injection. The intensity of the light and the movement of the carriers are necessary for this control — it is directly proportional to these two parameters, which are mainly concentrated at the tips of the pores, which serve as openings for the collection cavities. Consequently, the expansion produced by the etching process is constant and increased. The primary objective of our studies was to analyze the material's properties at low temperatures. In addition, we aimed to conduct an exhaustive study of the morphological and qualitative characteristics of the studied layers. Further research could investigate the relationship between optical and morphological properties. In addition, for semiconductor materials, the full width at half maximum (FWHM) of the PL emission spectrum can be used as a reliable measure to evaluate the material consistency. In this case, we have selected the initial peak with the highest intensity, corresponding to porous silicon, to determine the FWHM of the PL spectrum. The results are shown in Fig. 7. FWHM of the peaks remains relatively stable despite temperature variations, which indicates the consistency of the hole size within the fabricated porous layers. A lower FWHM value indicates that the material has a narrower size distribution and is also characterized by increased uniformity. Conversely, a higher FWHM value indicates that the substance has a wider range of sizes and is less uniform [42].

4. Conclusions

Conducting photoluminescence spectroscopy tests on N-type porous silicon at different temperatures can provide a thorough understanding of the properties of charge carriers, defects, and surface interactions. This study investigates the changes in photoluminescence properties of porous silicon sheets in response to temperature variations. The investigation involves the study of photoluminescence spectra that vary with temperature and time. These spectra were measured in a temperature range from 10 to 300 K. Using an N-type material, the porous silicon was used to construct the temperature-dependent integrated PL intensity and PL decay curves to examine the mechanisms of PL quenching. These studies provided a crucial understanding of the photoluminescence phenomena exhibited by porous silicon by studying the low-temperature photoluminescence with time resolution. It can be concluded that carrier redistribution at the surface is primarily responsible for photoluminescence emission in porous materials. The electrical properties of the porous silicon layer may differ depending on the N-type substrate chosen. The presence and properties of dopants in the substrate and the porous silicon can affect the movement, concentration, and combination rates of charge carriers, as well as the photoluminescence brightness. A complex interplay of temperature-dependent events is observed in the porous silicon layer derived from an N-type silicon substrate. Researchers often study this behavior, which changes with temperature, to understand the material's properties, including its defect properties, quantum confinement effects, electrical structure, and much more. In-depth studies of the electrical, structural, and photoluminescence properties at different temperatures provide important new information about the special properties of porous silicon and its possible applications in optoelectronics and other industries. Various materials' electrical and optical properties can be effectively analyzed by studying photoluminescence at low temperatures. These investigations are crucial for improving the effectiveness of porous silicon in various applications, including sensors, light-emitting devices, optoelectronic devices, and photodetectors.

References

[1] R. Vercauteren, G. Scheen, J.-P. Raskin, L.A. Francis, *Sens. Actuators A Phys.* **318**, 112486 (2020).

[2] D. Dovzhenko, I. Martynov, P. Samokhvalov, E. Osipov, M. Lednev, A. Chistyakov, A. Karaulov, I. Nabiev, *Opt. Express* **28**, 22705 (2020).

[3] T. Thomas, Y. Kumar, J.A.R. Ramón, V. Agarwal, S.S. Guzmán, R. Reshmi, S. Pushpan, S.L. Loredo, K.C. Sanal, *Vacuum* **184**, 109983 (2021).

[4] D. Yan, S. Xia, S. Li, S. Wang, M. Tan, S. Liu, *Mater. Res. Bull.* **134**, 111109 (2021).

[5] M.H. Kareem, A.M.A. Hussein, H.T. Hussein, *J. Mech. Behav. Mater.* **30**, 257 (2021).

[6] C.W. Ferreira, R. Vercauteren, L.A. Francis, *Micromachines* **13**, 10 (2021).

[7] L.T. Canham in: *Porous Silicon for Biomedical Applications*, Ed. H.A. Santos, Elsevier, 2014, p. 3.

[8] V.M. Rotshteyn, T.K. Turdaliev, K.B. Ashurov, *Appl. Sol. Energy* **57**, 480 (2021).

[9] S. Rahmouni, L. Zighed, S. Chaguetmi et al., *Optoelectron. Adv. Mater.* **12**, 553 (2018).

[10] S. Rahmouni, N. Boukhanoufa, I. Tifouti, H. Bendjeffal, B. Mariane, *Silicon* **15**, 3261 (2023).

[11] Y. Afandi, G. Parish, A. Keating, *Mater. Sci. Semicond. Process.* **138**, 106314 (2022).

[12] S. Sharma, K.K. Jain, A. Sharma, *Mater. Sci. Appl.* **6**, 1145 (2015).

[13] J.M. Lauerhaas, G.M. Credo, J.L. Heinrich, M.J. Sailor, *J. Am. Chem. Soc.* **114**, 1911 (1992).

[14] M.A. Almeshaal, B. Abdouli, K. Choubani, L. Khezami, M.B. Rabha, *Silicon* **15**, 6025 (2023).

[15] F.K. Başak, E. Kayahan, *Opt. Mater.* **124**, 111990 (2022).

[16] Z. Yan, J. Jiang, Y. Zhang, D. Yang, N. Du, *Mater. Today Nano* **18**, 100175 (2022).

[17] L.T. Canham, *Appl. Phys. Lett.* **57**, 1046 (1990).

[18] R. Ramadan, R.J. Martín-Palma, *Nanomaterials* **12**, 271 (2022).

[19] M. Rahmani, S. Amdouni, M.-A. Zaibi, A. Meftah, *J. Mater. Sci. Mater. Electron.* **32**, 4321 (2021).

[20] F.I.H. Rhouma, F. Belkhiria, E. Bouzaiene, M. Daoudi, K. Taibi, J. Dhahri, R. Chtourou, *RSC Adv.* **9**, 5206 (2019).

[21] P. Elia, E. Nativ-Roth, Y. Zeiri, Z. Porat, *Microporous Mesoporous Mater.* **225**, 465 (2016).

[22] M. Szymura, M. Duda, M. Karpińska, T. Kazimierczuk, R. Minikayev, K. Sobczak, M. Parlińska-Wojtan, *J. Phys. Chem. C* **127**, 6768 (2023).

[23] E.C. Larkins, J.S. Harris Jr., in: *Molecular Beam Epitaxy: Applications to Key Materials*, Ed. R.F.C. Farrow, Noyes, Park Ridge (NJ) 1995, p. 114.

[24] S. Burkner, J.D. Ralston, S. Weisser, J. Rosenzweig, E.C. Larkins, R.E. Sah, J. Fleissner, *IEEE Photon. Technol. Lett.* **7**, 941 (1995).

[25] H. Diesinger, A. Bsiesy, R. Hérino, B. Gelloz, *Mater. Sci. Eng. B* **69**, 167 (2000).

[26] S. Rahmouni, H. Boubekri, H. Bendjeffal et al., *Silicon* **16**, 4253 (2024).

[27] M. Çadırcı, *J. Lumin.* **228**, 117551 (2020).

[28] R.C. Egeberg, E. Veje, A. Ferreira Da Silva, I. Pepe, A. Santos Alves, *J. Porous Mater.* **7**, 173 (2000).

[29] W. Lu, A.T. Tarekegne, Y. Ou, S. Kamiyama, H. Ou, *Sci. Rep.* **9**, 16333 (2019).

[30] H. Rinnert, O. Jambois, M. Vergnat, *J. Appl. Phys.* **106**, 023501 (2009).

[31] Q. Yuan, B. Liang, C. Zhou, Y. Wang, Y. Guo, S. Wang, G. Fu, Y.I. Mazur, M.E. Ware, G.J. Salamo, *Nanoscale. Res. Lett.* **13**, 387 (2018).

[32] H. Cheng, Y. Feng, Y. Fu, Y. Zheng, Y. Shao, Y. Bai, *J. Mater. Chem. C* **10**, 13590 (2022).

[33] A. Mabrouk, N. Lorrain, M.L. Haji, M. Oueslati, *Superlattices Microstruct.* **77**, 219 (2015).

[34] G.-E. Weng, B.-P. Zhang, M.-M. Liang et al., *Funct. Mater. Lett.* **06**, 1350021 (2013).

[35] D. Zhao, B. Li, C. Wu, Y.-M. Lu, D. Shen, J. Zhang, X. Fan, *J. Lumin.* **119–120**, 304 (2006).

[36] S. Kobayashi, R. Akiyama, T. Furuta, M. Moriwaki, *Molecules Online* **2**, 35 (1998).

[37] S. Ten, F. Henneberger, M. Rabe, N. Peyghambarian, *Phys. Rev. B* **53**, 12637 (1996).

[38] H. Jin, L.-G. Zhang, Z.-H. Zheng, L.-N. An, Y.-M. Lu, J.-Y. Zhang, X.-W. Fan, D.-Z. Shen, *Chin. Phys. Lett.* **22**, 1518 (2005).

[39] M.V. Maximov, A.M. Nadtochiy, S.A. Mintairov et al., *Appl. Sci.* **10**, 1038 (2020).

[40] J. Toulouse, *J. Light. Technol.* **23**, 3625 (2005).

[41] M.A. Fakhri, B.G. Rashid, N.H. Numan, B.A. Bader, F.G. Khalid, T.A. Zaker, E.T. Salim, *AIP Conf. Proc.* **2045**, 020016 (2018).

[42] S.A. Abdulgafar, Y.M. Hassan, M.A. Ibrahem, *J. Mater. Sci. Mater. Electron.* **34**, 979 (2023).